SPANDIDOS PUBLICATIONS

INTERNATIONAL JOURNAL OF ONCOLOGY 56: 794-806, 2020

H19/let-7/Lin28 ceRNA network mediates autophagy inhibiting epithelial-mesenchymal transition in breast cancer

HANCHU XIONG[1,2*], JIANGUO SHEN[1,2*], ZIHAN CHEN[3*], JINGJING YANG[1,2], BOJIAN XIE[4], YUNLU JIA[1,2], USHANI JAYASINGHE[5], JI WANG[1,2], WENHE ZHAO[1,2], SHUDUO XIE[1,2], LINBO WANG[1,2] and JICHUN ZHOU[1,2]

[1]Department of Surgical Oncology, Sir Run Run Shaw Hospital, Zhejiang University; [2]Biomedical Research Center and Key Laboratory of Biotherapy of Zhejiang Province; [3]Department of Surgical Intensive Care Unit, First Affiliated Hospital, Zhejiang University, Hangzhou, Zhejiang 310016; [4]Department of Surgical Oncology, Taizhou Hospital, Taizhou, Zhejiang 318000, P.R. China; [5]Department of Surgical Oncology, Rhode Island Hospital, Brown University, Providence, RI 02912, USA

Received September 7, 2019; Accepted December 23, 2019

DOI: 10.3892/ijo.2020.4967

Abstract. Long non-coding RNA (lncRNA) H19 and Lin28 protein have been shown to participate in various pathophysiological processes, including cellular proliferation, autophagy and epithelial-mesenchymal transition (EMT). A number of studies have investigated lncRNAs, microRNAs and mRNAs, and their roles in the initiation and progression of cancer, in doing so identifying competitive endogenous RNA (ceRNA) networks, including the H19/let-7/Lin28 network. However, whether the H19/let-7/Lin28 ceRNA network is involved in autophagy and EMT in breast cancer (BC) remains unclear. The present study demonstrated that the H19/let-7/Lin28 loop was required for the downregulation of autophagy in BC cells via western blot analysis, reverse transcription-quantitative PCR and autophagy flux monitoring. Using wound healing, migration and invasion assays, and morphological assays, the H19/let-7/Lin28 loop was revealed to promote EMT in BC cells. Moreover, the H19/let-7/Lin28 network was found to contribute to autophagy by inhibiting EMT in BC cells. To the best of our knowledge, the present study is the first to suggest the important roles of the H19/let-7/Lin28 ceRNA network in BC autophagy and EMT, thus providing insight for the use of these molecules as prognostic biomarkers and therapeutic targets in BC metastasis.

Correspondence to: Professor Linbo Wang or Dr Jichun Zhou, Department of Surgical Oncology, Sir Run Run Shaw Hospital, Zhejiang University, 3 Qingchun East Road, Hangzhou, Zhejiang 310016, P.R. China
E-mail: linbowang@zju.edu.cn
E-mail: jichun-zhou@zju.edu.cn

*Contributed equally

Key words: H19, Lin28, breast cancer, autophagy, epithelial-mesenchymal transition, competing endogenous RNA

Introduction

Breast cancer (BC) is one of the leading causes of cancer-associated mortality in females ≤40 years of age globally (1). Early detection and comprehensive treatment, which currently consist of surgery, radiation, chemotherapy, endocrine therapy and targeted therapy, have substantially improved the prognosis of patients with BC (2). Nevertheless, a significant proportion of patients still develop distant metastases, and their prognoses remain poor (3). Moreover, the use of conventional therapies has not increased the overall survival of patients with metastatic BC (4). Therefore, to determine the potential molecular mechanisms underlying BC metastasis, it is necessary to further investigate effective biomarkers and molecular targets for the disease.

The majority of the human genome can be transcribed into long non-coding RNAs (lncRNAs), which are transcripts >200 nucleotides in length. lncRNAs have attracted increasing attention for their critical roles in tumor biology, including those in tumor initiation and progression (5). First identified in 1991 by Bartolomei *et al* (6), lncRNA H19 has now been established as an oncogenic marker in a diverse range of cancer types, including liver, lung, gastric, bladder, pancreatic and colorectal cancers, as well as BC (7). Although H19 is considered an important therapeutic target for various diseases, the mechanisms and functions of H19 in BC remain poorly understood. Lin28, an RNA-binding protein and transcription factor, has drawn considerable attention due to its implicated involved in stem cell differentiation, normal development, glucose metabolism and cancer (8). Lin28 is frequently upregulated in BC, and functions as a oncogene in numerous cancer-associated processes (9).

Epithelial-mesenchymal transition (EMT) is the complete trans-differentiation from a functional epithelial cell to a mesenchymal-like cell, and involves multiple molecular signal transduction pathways (10). Numerous observations have indicated that autophagy-related regulatory pathways, such as the PI3K/AKT/mTOR and beclin-1 pathways, can influence EMT (11,12). Therefore, further understanding of the specific regulatory mechanisms between EMT and autophagy

is required. Autophagy, literally defined as self-eating, is a process via which cells degrade and recycle cytoplasmic material within lysosomes (13). Aside from its role in homeostatic maintenance, autophagy has also been implicated in a diverse range of pathologies, including cancer. Autophagic inhibition of EMT has been identified in pancreatic cancer (14), BC (15) and gastric cancer (16), but the underlying mechanisms of autophagy in cancer cells remain controversial.

In the present study, the H19/let-7/Lin28 loop was found to be a requirement for downregulating autophagy in BC cells. Using Transwell and morphological assays, the H19/let-7/Lin28 loop was found to promote the EMT of BC cells. Moreover, the H19/let-7/Lin28 network was found to be involved in the autophagic inhibition of EMT in BC. Therefore, the results of the present study indicate that targeting the H19/let-7/Lin28 competitive endogenous RNA (ceRNA) network may provide putative prevention and treatment for the metastasis of BC.

Materials and methods

Ethics statement. All patients provided written informed consent for the use of the remainder of their pathological specimens for research purposes. The protocols used during the present study, and the use of human tissue, were approved by the Ethics Committee of the Sir Run Run Shaw Hospital affiliated with Zhejiang University, and conducted in full accordance with the ethical principles cited in the World Medical Association Declaration of Helsinki and local legislation.

Patient information. From January 2016 to December 2016, a total of 43 patients with BC (42-54 years old) at the Department of Surgical Oncology, Sir Run Run Shaw Hospital, Zhejiang University were included in this study. Of these patients, the 23 patients with lymph node (LN)-positive BC ranged from 42 to 54 years, and the 20 patients with LN-negative BC ranged from 44 to 54 years. Breast cancer tissues were surgically obtained from patients and frozen at -80˚C.

Cell lines, antibodies and chemical reagents. The SK-BR-3, MCF-7, MDA-231 and T-47D human BC cell lines, and the MCF-10A normal human breast cell line were obtained from the American Type Culture Collection (ATCC). MDA-231 cells were cultured in Leibovitz's L-15 medium (cat. no. 11415-064) and the other cell lines were cultured in RPMI-1640 medium (cat. no. 11875-093; both Invitrogen; Thermo Fisher Scientific, Inc.) supplemented with 10% fetal bovine serum (FBS; Gibco; Thermo Fisher Scientific, Inc.). All cells were incubated at 37˚C with 5% CO_2 and 95% humidity. The anti-Lin28 antibody (cat. no. 3533-1) was obtained from Epitomics (Abcam), and the anti-β-Actin antibody (cat. no. sc-47778) was purchased from Santa Cruz Biotechnology, Inc. The anti-GAPDH antibody (cat. no. 5174) and anti-β-Tubulin antibody (cat. no. 2146) were purchased from Cell Signaling Technology, Inc. Primary antibodies against the EMT markers E-cadherin (cat. no. 3195) and vimentin (cat. no. 5741) were purchased from Cell Signaling Technology, Inc. Of the autophagy markers, anti-p62 (cat. no. PM045) was purchased from MBL International Co., anti-beclin-1 (cat. no. 3495) was purchased from Cell Signaling Technology, Inc. and microtubule-associated protein light chain (LC)3B (cat. no. L7543) was acquired from Sigma-Aldrich (Merck KGaA). For autophagy induction, cells were treated with 200 nM rapamycin (Rapa; cat. no. 37094; Sigma-Aldrich; Merck KGaA). For autophagy inhibition, the cells were treated with 50 μM chloroquine (CQ; cat. no. C6628; Sigma-Aldrich; Merck KGaA). All cells were incubated at 37˚C for 24 h during treatment with these compounds. For the morphological change assays, the cells were treated with 2.5 ng/ml transforming growth factor (TGF)-β (R&D Systems, Inc.) for 24 h at 37˚C. Each sample was observed under a Zeiss LSM 710 confocal microscope (magnification, x100).

Stable Lin28-expressing SK-BR-3 cell line. Third-generation Lin28 lentiviral vectors were generated with the LV-LIN28A plasmid (Addgene, Inc.) and vesicular stomatitis virus G (Addgene, Inc.), and then transiently transfected into $2.5x10^5$ 293T (ATCC) cells at a ratio of 6:1 using Lipofectamine® 3000 transfection reagent (cat. no. L3000001; Invitrogen; Thermo Fisher Scientific, Inc.), according to the manufacturer's protocol; viral supernatants were collected 36 h later and filtered through a 0.45-μm filter. After $5x10^4$ SK-BR-3 cells were inoculated into 48-well plates for 24 h, viral supernatants (MOI=5) and diethyl-aminoethyl (DEAE)-dextran (20 μg/ml; Baomanbio, Inc.) were added into the plate. After culturing for 12 h, the original medium was replaced with DMEM (Gibco; Thermo Fisher Scientific, Inc.) containing 10% FBS for culture for another 72 h. After cells were screened using puromycin (Sigma-Aldrich; Merck KGaA) and cloned, the SK-BR-3 cell lines exhibiting stable infection were selected. Overexpression of Lin28 was then verified via western blotting; clone 1 and 24 (S1 and S24) were found to exhibit stable expression of Lin28.

RNA/microRNA (miRNA/miR) extraction and reverse transcription-quantitative (RT-q)PCR. Total RNA was extracted from tissue specimens using an miRNeasy FFPE Kit (cat. no. 217504; Qiagen, Inc.), and was isolated from cell lines using an E.Z.N.A.® Total RNA Kit I (cat. no. R6834-02; Omega Bio-Tek, Inc.) according to the manufacturer's protocols. All samples were eluted in 50 μl diethyl pyrocarbonate water. RNA was quantified using a NanoDrop™ 2000c (NanoDrop Technologies; Thermo Fisher Scientific, Inc.). RT reactions were performed using random primers from a HiFiScript cDNA Synthesis Kit (cat. no. CW2569-100; Beijing CoWin Biotech Co., Ltd.) according to the manufacturer's protocol. Relative mRNA expression levels were determined via qPCR (initial denaturation at 95˚C for 30 sec, followed by 40 cycles at 95˚C for 5 sec and 60˚C for 34 sec) using SYBR® Green Master Mix (cat. no. CW0957M; Beijing CoWin Biotech Co., Ltd.) and an ABI 7500 Real-Time PCR System (Applied Biosystems; Thermo Fisher Scientific, Inc.). Tubulin was used as an internal control for mRNA expression. For miRNA quantification, RT-qPCR was performed using a Bulge-loop™ miRNA qRT-PCR Starter Kit (cat. no. C10211-2; Guangzhou RiboBio Co., Ltd.) according to the manufacturer's instructions; the kit included let-7a and U6 primers (cat. nos. S160726154727 and S1 60325154310; Guangzhou RiboBio Co., Ltd.), the latter of which was used as an internal control for miRNA expression. All other primers were purchased from Sangon Biotech Co., Ltd., and their sequences are listed in Table I. Relative RNA expression levels were calculated using the $2^{-\Delta\Delta Cq}$ method (17).

Table I. Primers used for quantitative PCR.

Gene	Primer sequence
H19	F: 5'-ACTCAGGAATCGGCTCTGGAA-3'
	R: 5'-CTGCTGTTCCGATGGTGTCTT-3'
Lin28	F: 5'-AGCGCAGATCAAAAGGAGACA-3'
	R: 5'-CCTCTCGAAAGTAGGTTGGCT-3'
Tubulin	F: 5'-CGTGTTCGGCCAGAGTGGTGC-3'
	R: 5'-GGGTGAGGGCATGACGCTGAA-3'
β-catenin	F: 5'-GATACCTCCCAAGTCCTGTATGAG-3'
	R: 5'-GCATCAAACTGTGTAGATGGGATC-3'
ZEB1	F: 5'-CGCGTCCCTACGGTTTC-3'
	R: 5'-CAACCACCACCACATGTTCAG-3'
Twist	F: 5'-TTCAAAGAAACAGGGCGTGG-3'
	R: 5'-CCGTCTGGGAATCACTGTCC-3'
Snail	F: 5'-CATCCTTCTCACTGCCATGGA-3'
	R: 5'-AGGCAGAGGACACAGAACCAGA-3'
Slug	F: 5'-AGACCCCCATGCCATTGAAG-3'
	R: 5'-GGCCAGCCCAGAAAAAGTTG-3'
HMGA2	F: 5'-CGAAAGGTGCTGGGCAGCTCCGG-3'
	R: 5'-CCATTTCCTAGGTCTGCCTCTTG-3'
Beclin-1	F: 5'-GGCTGAGAGACTGGATCAGG-3'
	R: 5'-CTGCGTCTGGGCATAACG-3'
p62	F: 5'-AAGTCAGCAAACCTGACG-3'
	R: 5'-CCATCTGTTCCTCTGGCT-3'

F, forward; R, reverse; ZEB1, zinc finger E-box binding homeobox 1; HMGA2, high-mobility group AT-hook 2.

Plasmids. pH19 and its corresponding mutant plasmid (pH19mut) were synthesized as previously described (18), with the 2.6-kb-long amplified H19 sequences inserted into pFLAG-CMV-2 vectors (Sigma-Aldrich; Merck KGaA). The sequences of wild-type and mutant human H19 are listed in Table II.

Small interfering (si)RNAs, miRNA mimics and inhibitors, and transfection. H19-siRNA (cat. no. 4390771), let-7 mimics (cat. nos. 4464066) and the control (cat. nos. AM17110), let-7 inhibitors (cat. nos. AM17000) and the control (cat. nos. 4464076) were synthesized by Ambion (Thermo Fisher Scientific, Inc.). Control siRNA and siLin28 sequences were synthesized by Guangzhou RiboBio Co., Ltd. (cat. nos. siN05815122147 and siG10118110813). A total of 3-5x10^5 cells/well were seeded into 24-well plates and incubated at 37˚C (5% CO_2) overnight. The cells were transfected with siRNA (10 μM), miRNA mimics or inhibitors (5 nM) using siPORT™ NeoFX™ transfection agent (cat. no. AM4511; Invitrogen; Thermo Fisher Scientific, Inc.); the corresponding negative controls (siRNA, miRNA mimics or inhibitors) were supplied by the manufacturers. For plasmid transfection, an equivalent number of cells were seeded into 24-well plates and incubated overnight; the cells were transfected with 1-2 μg of each plasmid using Lipofectamine 3000 transfection reagent, and empty vector was used as the negative control. The mRNA expression levels of H19, Lin28 and let-7 were determined by RT-qPCR 48 h post-transfection, and protein expression was determined by western blot analysis 72 h post-transfection.

Wound healing, migration and invasion assays. For the wound-healing assays, 5x10^5 cells were seeded into 6-well plates in triplicate. After 24 h (37˚C, 5% CO_2), a linear scratch was created across each monolayer using a sterile pipette tip. The cells were then washed twice with PBS and incubated in serum-free medium for 24 h, and the wound widths were measured at 0, 24 and 48 h.

Cell migration was assessed using Millicell® Hanging Cell Culture Inserts in 24-well plates (EMD Millipore) according to the manufacturer's instructions. Briefly, serum-free medium containing 2x10^5 cells from each subgroup was added to the upper chamber, and 600 μl medium containing 10% FBS was added to the lower chamber as a chemoattractant. The cells were incubated for 24 h at 37˚C (5% CO_2).

For the invasion assay, the same procedure was used as for the cell migration assay, but the filters were pre-coated with 100 μl Matrigel (BD Biosciences) at a 1:3 dilution in medium; the cells were then incubated for 48 h at 37˚C (5% CO_2). Following incubation, the cells on the upper surface of the membrane were removed using a cotton swab; cells that had migrated to or invaded the lower membrane were fixed in methanol for 15 min, and subsequently stained with 0.05% crystal violet in PBS for 15 min (both at room temperature). Migration and invasion were assessed by counting the number of stained cells from 10 random fields per filter in each group under a light microscope (magnification, x20; Olympus Corporation). The results are depicted as the mean ± SD, and each experiment was conducted in triplicate and repeated ≥3 times.

Western blot analysis. Cultured cells were lysed using RIPA buffer (Pierce; Thermo Fisher Scientific, Inc.) containing a protease inhibitor cocktail (Roche Diagnostics). The protein concentration of the lysates was measured using a Protein Assay Kit II (cat. no. 500-0002EDU; Bio-Rad Laboratories, Inc.). Equivalent amounts of protein (10 μl) were resolved and mixed with 5X Lane Marker Reducing Sample Buffer (Pierce; Thermo Fisher Scientific, Inc.) prior to SDS-PAGE (12%). The proteins were transferred to PVDF membranes (EMD Millipore) and blocked with 5% non-fat milk for 1 h at 20˚C. The membranes were then probed with the aforementioned primary antibodies (all 1:1,000), washed with TBS-0.1% Tween-20 and subsequently incubated with corresponding horseradish peroxidase-conjugated secondary antibodies (1:2,000; cat. nos. GAM0072 and GAR0072; MultiSciences Biotech Ltd.). The protein bands were developed using an enhanced chemiluminescent detection system (Bio-Rad Laboratories, Inc.). All experiments were conducted in triplicate.

Cell viability assay. Cells were harvested and seeded into 96-well plates (4x10^3/well) in triplicate. After culturing for 2 days, 20 μl MTT (Amresco, LLC) was added to each well and the cells were incubated for a further 4 h at 37˚C. The optical density was determined at least in triplicate against a reagent blank (wavelength, 490 nm) using a spectrophotometric microplate reader.

Table II. Sequences of wild-type and mutant human H19.

H19 version	Sequence (5'-3')
Wild-type	GTAGGACGAAGCTGGGGGAGGGTCACAGGGATGCCACCCGGGATCCGTAACAGTGTTTATTGATG ATGAGTCCAGGGCTCCTGCTGAAGCCCTGGTGGGGAGGGGCACAGAGCGAGATGGGGCGTAATG GAATGCTTGAAGGCTGCTCCGTGATGTCGGTCGGAGCTTCCAGACTAGGCGAGGGCAGGGTGAGG CCTCGGGCACACAGCCGGCGCCCAGTCACCCGGCCCAGATGGAGGGCGGCCGGGCCCTGCACAG GCACTTGCCAAGGTGGCTCACACTCACGCACACTCGTACTGAGACTCAAGGCCGTCTCCACAACT CCAACCAGTGCAAATGACTTAGTGCAAATTAAATTCAGAAGGGACGGGGGAAACAGAGTCGTGGA GGCTTTGAATCTCTCAGAAAAAAGGAAAGACAGGAAAGCTCAGAAACAAAGAGACAGAAGGATG AAAAAGAAGAAGAGGGAGGTGGTGGGGACGGCGTCATCCCGCTGGAGGAGCTCAGCTCTGGGAT GATGTGGTGGCTGGTGGTCAACCGTCCGCCGCAGGGGGTGGCCATGAAGATGGAGTCGCCGGTGC GGGGTGGGTGCTGCGGGCGCCGCTGTTCCGATGGTGTCTTTGATGTTGGGCTGATGAGGTCTGGTT CCTCTAGCTTCACCTTCCAGAGCCGATTCCTGAGTCAGGTAGTGCAGTGGTTGTAAAGTGCAGCAT ATTCATTTCCAAGCTAGAGGGTTTTGTGTCCGGATTCAAAGGCCCAGGCTTGAGCTGGGTAGCACC ATTTCTTTCATGTTGTGGGTTCTGGGAGCCCAGAGGGCAGCCATAGTGTGCCGACTCCGTGGAGGA AGTAAAGAAACAGACCCGCTTCTTGCCGCAGCCCCACCAGCCTAAGGTGTTCAGGAAGGCCGGAC GCGCCTCCTCTGTCCTCGCCGTCACACCGGACCATGTCATGTCCTGCTTGTCACGTCCACCGGACC TGGCGTCTTGGCCTTCGGCAGCTGGTGGGCACGTCCACCCCAGCTGGAGACCTGGCCTCGTCTCCA GCCCGAACGCTGAGGCACCGATCCCGGCTCCGTCGCCGCCCGCGAGGCCCGCCTTGGCCACGGGC TCTGGAGGCCAGTGCCTCCCGCTCGCCGCCCGCTGCGCTCCTCACCCCTGCCTGCACCATCCTCCC TCCTGAGAGCTCATTCACTCCGCCCCGCCCGCCTCGCCTAGTCTGGTCTCGCCCCATGCCCTTGACT CCCCTGGATGCTGTACTGTCTGCCAAGCCAGCCCCAGGGGCTGAGCGGTGAGGGCATACAGCGTC ACCAAGTCCACTGTGGGCCCTCTCCGCACCAGACCCTGGGCCGCAGTGCCTCGTGGGACCGGCGC CCGCAGGCCGAGCCCCTGCAGCCTCCTTGCTGCGCAATGTCCCGGGGCCCCCCTCCCGTGGCCGCT TCGCCCTCCTGGTGACGTCCTGCTGCAACTCCCCGAGCACTGCCTGTCTTCCCGCTCTCCAGCCCT CGAGGCTCCTGTGCCTGCTACTAAATGAATTGCGGTGGGTGAGGTGGCAGCTGGGGACCCCTCTGT CCTGTGTCCCCTGCCATGTCCCTGTCTGACCCAGGCCTGGGGTACCACCCCACGTGCTGGACCCTA CGCTAGCCACCCCTGTGCTCCCTCCCTGCCCTCTTGCTCTTTCTGCCTGGAACGGGCCCATAACCCC CCAGCCTTGCGCAGTCTCGGCTCCCCCCGAGAAGATGTCACCTTTGCTAACTCTCCTGCCCCCATCC TGCCCCTCTGCTGGGAGGGTGTCTGCTTCTCCCCGCCAGCCCTCGATCCCCTAAACCTCCTTCTTTC AGAAGGCTGGGGAAGCGAGGCCTGGGGAGGGAAGGGACTCACCTGCCCGGCAGATGGGGTCCTC ACCTGCCCGCTGCTGCCAGCTACACCTCCGTTGCCCAGGCCCTGGGATCAAACCCTGCCCACCAGC TCCCCTCGTCCAACCAGCTGCCACGTCCTGTAACCAAAAGTGACCGGGATGAATGCCTGGCTCCCC CTTCTTTCCAGCCCTAGCTCAGGCCCATCGTCCCCAGCTGATGTCGCCCTGTCTGCACGATGCCTGG GCGCCTACTCCACACTCCTCACTGGCCTCAGGCCCCACCAGCCCTGCCTCGAGCTAGCCCCTCCAC CCGTCATCACTCCTGCCAGACTCCAGATGTCCAAGGTGCTCCTTGGCTCCCACAAGCTCTCCTCCA GCACCCCATCTTCCCCTGGTTGCCCCTCGGTTCCCCACTTCCCCAGTTTCCCCCGTTACCCCCCACC CATCCCACCCCCTCCCTCACCCTGCTGCGGCCGCAAGCTTGTCGTCATCGTCTTTGTAGTCCATGGT AGATCAATTCTGACGGTTCACTAAACGAGCTCTGCTTATATAGACCTCCCACCGTACACGCCTACCG CCCATTTGCGTCAACGGGGCGGGGTTATTACGACATTTTGGAAAGTCCCGTTGATTTTGGTGCCAAA ACAAACTCCCATTGACGTCAATGGGGTGGAGACTTGGAAATCCCCGTGAGTCAAACCGCTATCCAC GCCCATTGGTGTACTGCCAAAACCGCATCACCATGGTAATAGCGATGACTAATACGTAGATGTACTG CCAAGTAGGAAAGTCCCGTAAGGTCATGTACTGGGCATAATGCCAGGCGGGCCATTTACCGTCATT GACGTCAATAGGGGGCGGACTTGGCATATGATACACTTGATGTACTGCCAAGTGGGCAGTTTACCG TAAATACTCCACCCATTGACGTCAATGGAAAGTCCCTATTGGCGTTACTATGGGAACATACGTCATT ATTGACGTCAATGGGCGGGGGTCGTTGGGCGGTCAGCCAGGCGGGCCATTTACCGTAAGTTATGTA ACGCGGAACTCCATATATGGGCTATGAACTAATGACCCCGTAATTGATTACTATTAATAACTAGTCAA TAATCAATGTCAACATGGCGGTCATATTGGACATGAGCCAATATAAATGTACATAT
Mutant	GCGGACGAGGAATGGGGAGGGGTCACAGGGATGCCACCCGGGATCCGTAACAGTGTTTATTGATG ATGAGTCCAGGGCTCCTGCTGAAGCCCTGGTGGGGAGGGGCACAGAGCGAGATGGGGCGTAATG GAATGCTTGAAGGCTGCTCCGTGATGTCGGTCGGAGCTTCCAGACTAGGCGAGGGCAGGGTGAAA GTGCTATAAGTGCAGGTGCGCCCAGTCACCCGGCCCAGATGGAGGGCGGCCGGGCCCTGCACAGG CACTTGCCAAGGTGGCTCACACTCACGCACACTCGTACTGAGACTCAAGGCCGTCTCCACAACTC CAACCAGTGCAAATGACTTAGTGCAAATTAAATTCAGAAGGGACGGGGGAAACAGAGTCGTGGAG

Table II. Continued.

H19 version	Sequence (5'-3')
	GCTTTGAATCTCTCAGAAAAAAGGAAAGACAGGAAAGCTCAGAAACAAAGAGACAGAAGGATGA
	AAAAGAAGAAGAGGGAGGTGGTGGGGACGGCGTCATCCCGCTGGAGGAGCTCAGCTCTGGGATG
	ATGTGGTGGCTGGTGGTCAACCGTCCGCCGCAGGGGGTGGCCATGAAGATGGAGTCGCCGGTGCG
	GGGTGGGTGCTGCGGGCGCCGCTGTTCCGATGGTGTCTTTGATACGACGCTGATGAGGTCTGGTTC
	CTCTAGCTTCACCTTCCAGAGCCGATTCCTGAGTCAAAGTGCTATAAGTGCAGGTAGTGCAGCATA
	TTCATTTCCAAGCTAGAGGGTTTTGTGTCCGGATTCAAAGGCCCAGGCTTGAGCTGGGTAGCACCA
	TTTCTTTCATGTTGTGGGTTCTGGGAGCCCAGAGGGCAGCCATAGTGTGCCGACTCCGTGGAGGAA
	GTAAAGAAACAGACCCGCTTCTTGCCGCAGCCCCACCAGCCTAAGGTGTTCAGGAAGGCCGGACG
	CGCCTCCTCTGTCCTCGCCGTCACACCGGACCATGTCATGTCCTGCTTGTCACGTCCACCGGACCT
	GGCGTCTTGGCCTTCGGCAGCTGGTGGGCACGTCCACCCCAGCTGGAGACCTGGCCTCGTCTCCA
	GCCCGAACGCTAAAGTGCTATAAGTGCAGGTGTCGCCGCCCGCGAGGCCCGCCTTGGCCACGGGC
	TCTGGAGGCCAGTGCCTCCCGCTCGCCGCCCGCTGCGCTCCTCACCCCTGCCTGCACCATCCTCCC
	TCCTGAGAGCTCATTCACTCCGCCCCGCCCGCCTCGCCTAGTCTGGTCTCGCCCCATGCCCTTGAC
	TCCCCTGGATGCTGTACTGTCTGCCAAGCCAGCCCCAGGGGCTGAGCGGTGAGGGCATACAGCGT
	CACCAAGTCCACTGTGGGCCCTCTCCGCACCAGACCCTGGGCCGCAGTGCCTCGTGGGACCGGCG
	CCCGCAGGCCGAGCCCCTGCAGCCTCCTTGCTGCGCAATGTCCCGGGGCCCCCCTCCCGTGGCCG
	CTTCGCCCTCCTGGTGACGTCCTGCTGCAACTCCCCGAGCACTGCCTGTCTTCCCGCTCTCCAGCC
	CTCGAGGCTCCTGTGCCTGCTACTAAATGAATTGCGGTGGGTGAAAGTGCTATAAGTGCAGGTTCT
	GTCCTGTGTCCCCTGCCATGTCCCTGTCTGACCCAGGCCTGGGGTACCACCCCACGTGCTGGACCC
	TACGCTAGCCACCCCTGTGCTCCCTCCCTGCCCTCTTACTCTTTCTGCCTGGAACGGGCCCATAACC
	CCCCAGCCTTGCGCAGTCTCGGCTCCCCCCGAGAAGATGTCACCTTTGCTAACTCTCCTGCCCCCA
	TCCTGCCCCTCTGCTGGGAGGGTGTCTGCTTCTCCCCGCCAGCCCTCGATCCCCTAAACCTCCTTCT
	TTCAGAAGGCTGGGGAAGCGAGGCCTGGGGAGGGAAGGGACTCACCTGCCCGGCAGATGGGGTC
	CTCACCTGCCCGCTGCTGCCAGCTACACCTCCGTTGCCCAGGCCCTGGGATCAAACCCTGCCCACC
	AGCTCCCCTCGTCCAACCAGCTGCCACGTCCTGTAACCAAAAGTGACCGGGATGAATGCCTGGCTC
	CCCCTTCTTTCCAGCCCTAGCTCAGGCCCATCGTCCCCAGCTGATGTCGCCCTGTCTGCACGATGCC
	TGGGCGCCTACTCCACACTCCTCACTGGCCTCAGGCCCCACCAGCCCTGCCTCGAGCTAGCCCCTC
	CACCCGTCATCACTCCTGCCAGACTCCAGATGTCCAAGGTGCTCCTTGGCTCCCACAAGCTCTCCT
	CCAGCACCCCATCTTCCCCTGGTTGCCCCTCGGTTCCCCACTTCCCCAGTTTCCCCCGTTACCCCCC
	ACCCATCCCACCCCCTCCCTCACCCTGCTGCGGCCGCAAGCTTGTCGTCATCGTCTTTGTAGTCCAT
	GGTAGATCAATTCTGACGGTTCACTAAACGAGCTCTGCTTATATAGACCTCCCACCGTACACGCCTA
	CCGCCCATTTGCGTCAACGGGGCGGGGTTATTACGACATTTTGGAAAGTCCCGTTGATTTTGGTGCC
	AAAACAAACTCCCATTGACGTCAATGGGGTGGAGACTTGGAAATCCCCGTGAGTCAAACCGCTAT
	CCACGCCCATTGGTGTACTGCCAAAACCGCATCACCATGGTAATAGCGATGACTAATACGTAGATGT
	ACTGCCAAGTAGGAAAGTCCCGTAAGGTCATGTACTGGGCATAATGCCAGGCGGGCCATTTACCGT
	CATTGACGTCAATAGGGGGCGGACTTGGCATATGATACACTTGATGTACTGCCAAGTGGGCAGTTTA
	CCGTAAATACTCCACCCATTGACGTCAATGGAAAGTCCCTATTGGCGTTACTATGGGAACATACGTC
	ATTATTGACGTCAATGGGCGGGGGTCGTTGGGCGGTCAGCCAGGCGGGCCATTTACCGTAAGTTAT
	GTAACGCGGAACTCCATATATGGGCTATGAACTAATGACCCCGTAATTGATTACTATTAATAACTAGT
	CAATAATCAATGTCAACATGGCGGTCATATTGGACATGAGCCAATATAAATGTACATAT

Autophagy flux monitoring. To evaluate the formation of fluorescent LC3B puncta, p-mCherry-C1-EGFP-hLC3B (LC3B) was used to monitor autophagy flux; 48 h after LC3B co-transfection with siRNAs, the cells were washed with 1X PBS and immediately analyzed via confocal microscopy (magnification, x100). DAPI Staining Solution (5 mg/ml; cat. no. C1006; Beyotime Institute of Biotechnology) was used for immunofluorescence staining at room temperature for 5 min. Each sample was observed under a Zeiss LSM 710 confocal microscope and the images were processed using ZEN LE software 2.0 (both Carl Zeiss AG).

Bioinformatics analysis. The association and prognostic modules of bc-GenExMiner v4.2 (bcgenex.centregauducheau.fr) were used to evaluate the associations between the expression of H19 and Lin28, as well as their prognostic value in human BC.

Statistical analysis. Unless otherwise indicated, all data are presented as the mean ± SD. Statistical analyses were performed using SPSS software version 17.0 (SPSS, Inc.). Linear regression analysis and Pearson's correlation coefficient were used to investigate the relationship between the

expression levels of H19 and Lin28, and Kaplan-Meier analyses of H19 and Lin28 and log-rank tests were used to evaluate prognosis. The Mann-Whitney U test was used to compare the differences between two groups, and data were analyzed using Kruskal-Wallis with Dunn's multiple comparison test among three or more groups. All graphs were constructed using Prism 7 version 7.0a (GraphPad Software, Inc.).

Results

H19/Let-7/Lin28 ceRNA network in BC. The results of the present study showed that the mRNA expression levels of H19 and Lin28 were higher in BC tissues with LN metastasis than those without (Fig. 1A and B). Furthermore, linear regression analysis verified a significant positive relationship between H19 and Lin28 expression in BC tissue samples collected from 43 patients (Fig. 1C). Kaplan-Meier curves were generated using the bc-GenExMiner database, which revealed that increased levels of H19 and Lin28 expression were both significantly associated with poor survival time in BC (Fig. 1D and E); this was validated by a strong positive association between the data obtained from bc-GenExMiner (Fig. 1F). The expression levels of H19 and Lin28 were also significantly increased in BC cell lines (MDA-231, MCF-7, SK-BR-3 and T-47D) compared with normal breast cells (MCF-10A; Fig. 1G and H).

The T-47D cell line was selected to investigate the association between H19 and Lin28 in BC, as these cells expressed the highest levels of Lin28 among the cell lines investigated (Fig. 1I). In T-47D cells transfected with siLin28, the H19 expression level was significantly downregulated (Fig. 1J). For the two established SK-BR-3 clones (S1 and S24; Fig. 1K) (19), RT-qPCR showed that H19 expression was significantly increased when Lin28 was overexpressed (Fig. 1L). To test the influence of H19 on Lin28, T-47D cells were transfected with siH19, and a decrease in the level of Lin28 mRNA and protein expression was observed (Fig. 1M and N). In addition, Lin28 expression was examined in MDA-231 cells transfected with pFlag-CMV-H19, which revealed that the H19 plasmid resulted in the successful overexpression of Lin28 at both the mRNA and protein level (Fig. 1O and P).

It is known that a double-negative feedback loop exists between let-7 and its RNA-binding protein Lin28 (8), and the results of the current study are consistent with these findings. As presented in Fig. S1A and B, the overexpression of let-7 in T-47D cells significantly inhibited the expression of Lin28 at both the mRNA and protein level; furthermore, MDA-231 cells transfected with a let-7 inhibitor exhibited an upregulation in Lin28 expression (Fig. S1C and D). Moreover, compared with the mock control, let-7 expression was significantly downregulated at the mRNA level in S1 and S24 (Fig. S1E). In T-47D cells transfected with siLin28, let-7 mRNA expression was upregulated as a result of the decreased expression of Lin28 (Fig. S1F).

It has been suggested that H19 may act as a sponge to antagonize miRNA let-7 (20). Collectively, lncRNA H19, miRNA let-7 and the transcription factor Lin28 may potentially form a double-negative ceRNA network in BC.

H19/let-7/Lin28 loop is required for autophagy in BC cells. Western blotting was used to determine the role of H19 in the autophagic regulation of BC, which showed that the overexpression of H19 decreased the expression of autophagy-associated molecules (beclin-1 and LC3-II) in MDA-231 cells; conversely, H19 knockdown in T-47D cells led to the upregulation of beclin-1 and LC3-II, and the downregulation of p62 (Fig. 2A). Autophagy flux monitoring was then performed to verify the influence of H19 on autophagy. As shown in Fig. 2B, autophagy flux was decreased in MDA-231 cells overexpressing H19 and increased in siH19-transfected T-47D cells. A similar trend was observed for the influence of Lin28 on p62, beclin-1 and LC3-II (Fig. 2C). RT-qPCR and western blot analyses revealed that H19 and Lin28 expression was significantly upregulated by a let-7 inhibitor (Fig. 2D and E); these results further indicated that the H19/let-7/Lin28 loop may affect autophagy in T-47D cells (Fig. 2F and G).

To further investigate the impact of autophagy on the H19/let-7/Lin28 loop in BC, MDA-231 and T-47D cells were treated for 24 h with the autophagic inhibitor CQ and the autophagic stimulator Rapa. The results showed that CQ upregulated the expression of both H19 and Lin28 mRNA, but that Rapa had a negative impact on H19 and Lin28 (Fig. 2H-K), which was also demonstrated by the protein expression level of Lin28 in T-47D cells (Fig. 2L and M). Of note, CQ/Rapa could only induce significant changes in Lin28 mRNA expression in MDA-231 cells, not protein expression (data not shown). Finally, a rescue experiment was conducted by co-treating T-47D cells with both Rapa and let-7 inhibitor, the results of which indicated that the H19/let-7/Lin28 loop may be involved in Rapa-induced autophagy in BC cells (Fig. 2N and O).

H19/let-7/Lin28 loop promotes EMT in BC cells. A positive relationship was found between H19 and Lin28 expression, and LN metastasis (Fig. 1A and B); subsequently, the effects of H19 and Lin28 overexpression and knockdown on the migration and invasion of BC cells were explored. Transwell assays showed that in MDA-231 cells, H19 overexpression significantly promoted migration and invasion (Fig. 3A-D). H19 knockdown in T-47D cells significantly inhibited migration and invasion (Fig. 3E-H). Furthermore, the wound closure time was notably decreased by H19 overexpression (in MDA-231 cells) and increased by H19 knockdown (in T-47D cells), compared with the control cells (Fig. S2A).

The migration and invasion of SK-BR-3 cancer cell clones was also investigated; the results demonstrated that upregulation of Lin28 significantly promoted the migration and invasion of S24 cells compared with the mock control (Fig. 3I-L). Following Lin28 knockdown in T-47D cells, western blotting demonstrated that Lin28 expression was significantly reduced compared with negative control (Fig. 3M). As predicted, downregulated expression of Lin28 significantly attenuated the migration and invasion of T-47D cells (Fig. 3N-P). These results were supported by wound healing assays (Fig. S2B), and a rescue experiment further indicated that H19/let-7/Lin28 enhanced the migratory and invasive abilities of BC cells (Fig. S3A and B).

Moreover, morphological changes associated with EMT were observed in SK-BR-3 and T-47D cells; specifically, H19 overexpression and the upregulation of Lin28 by let-7 inhibitor contributed to EMT (based on the transition from a

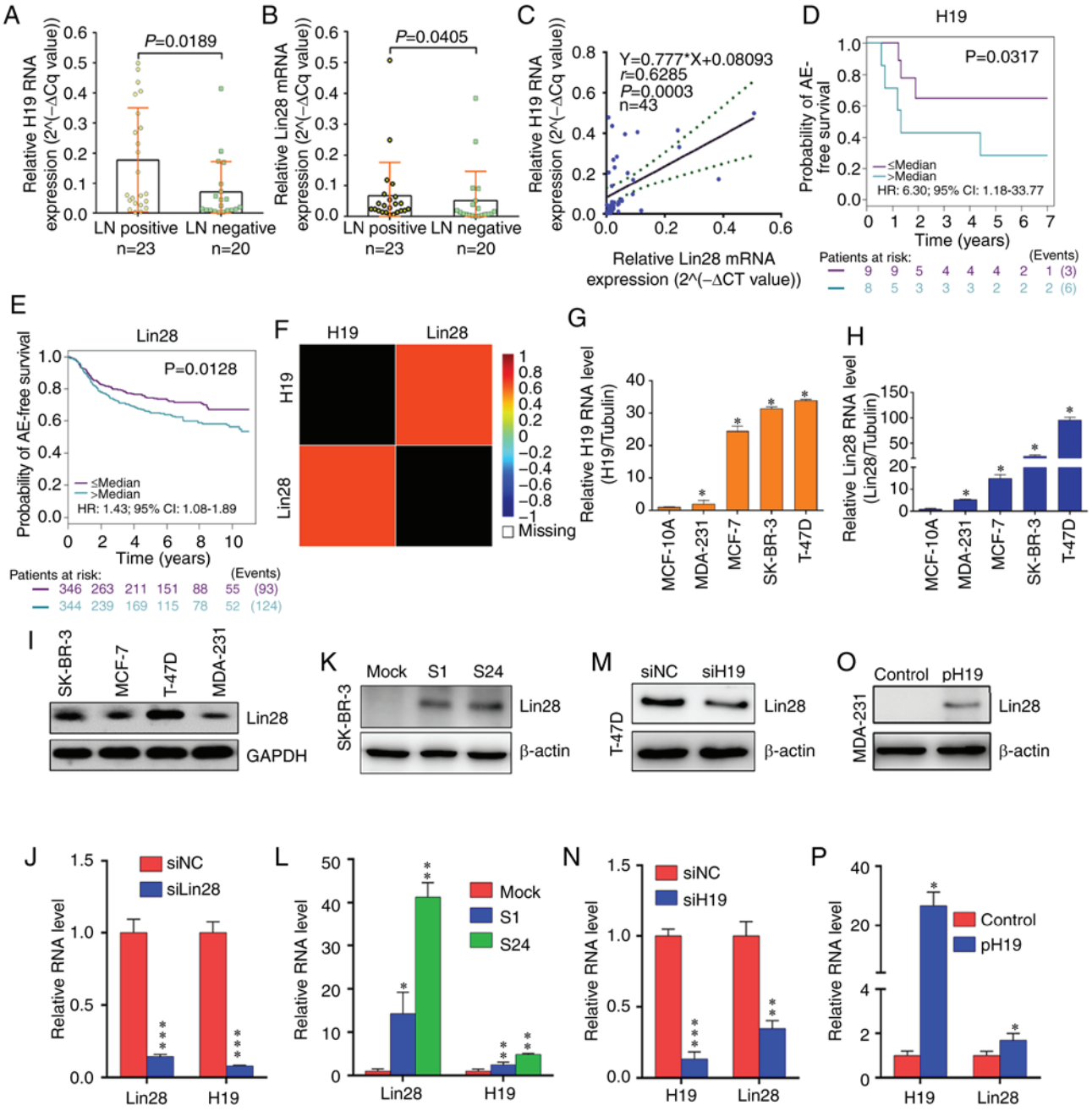

Figure 1. Upregulation of H19 and Lin28 indicates poor survival in BC. BC samples were divided into two groups based on clinical progression. (A) H19 and (B) Lin28 levels in the LN metastasis group (n=23) were significantly higher than those in the non-metastasis group (n=20). (C) Linear regression analysis indicated an *in vivo* positive relationship between the expression levels of H19 and Lin28 in a statistically significant manner. Pearson's correlation coefficient, P-value and sample size are indicated in the top left of the plot. Total RNA was subjected to RT-qPCR analysis; the Cq values were normalized to Tubulin in each sample. Kaplan-Meier survival curves of (D) H19 (P=0.0317) and (E) Lin28 (P=0.0128) were plotted using log-rank tests for patients with BC in the bc-GenExMiner v4.2 database. (F) Correlation map corresponding to the association between H19 and Lin28 expression was plotted for patients with BC in the bc-GenExMiner v4.2 database. The numbers represent Pearson's correlation coefficient. (G) H19 and (H) Lin28 levels were evaluated via RT-qPCR in four BC cell lines, and normal human MCF-10A breast cells were used as a control. *P<0.05 vs. MCF-10A. (I) Western blot analysis of Lin28 expression in four breast cancer cell lines. (J) RT-qPCR analysis of the RNA expression levels of Lin28 and H19 in T-47D cells transfected with siLin28. (K) Western blot analysis of Lin28 expression in SK-BR-3 cells S1 and S24. (L) RT-qPCR analysis of the RNA expression levels of Lin28 and H19 in SK-BR-3 cells S1 and S24; mock was used as a control. (M) Western blot analysis of Lin28 expression in T-47D cells transfected with siH19. (N) RT-qPCR analysis of the RNA expression levels of H19 and Lin28 in T-47D cells transfected with siH19. (O) Western blot analysis of Lin28 expression in MDA-231 cells transfected with pH19. (P) RT-qPCR analysis of the RNA expression levels of H19 and Lin28 in MDA-231 cells transfected with pH19. Results represent the mean ± SD of three independent experiments. *P<0.05, **P<0.01, ***P<0.001 vs. Control or Mock. BC, breast cancer; LN, lymph node; RT-qPCR, reverse transcription-quantitative PCR; Cq, quantification cycle; HR, hazard ratio; CI, confidence interval; si, small interfering RNA; NC, negative control; S1/S24, SK-BR-3 clones infected with a Lin28 overexpression lentivirus; pH19, pFlag-CMV-H19.

round cell morphology to a spindle-shaped morphology with antennae) after 24 h treatment (Fig. S4). To exclude the possibility that the aforementioned results were the consequence of Lin28 and H19 expression on the viability of BC cells, MTT assays were performed in cells following H19 or Lin28 upregulation/knockdown, which revealed that the metastatic

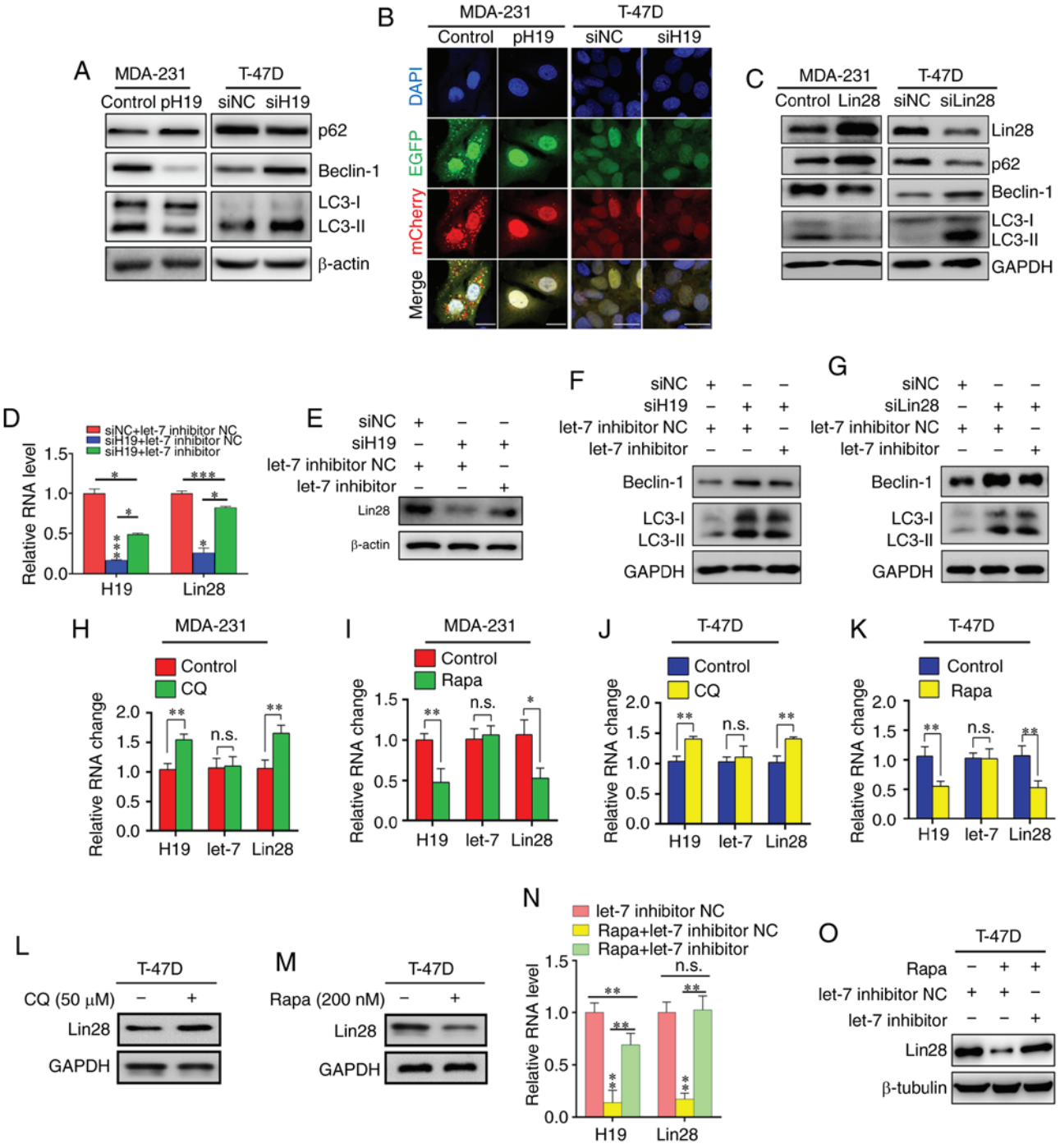

Figure 2. Reciprocal inhibition of the H19/let-7/Lin28 loop and autophagy in breast cancer cells. (A) Western blot analysis of autophagy marker expression in MDA-231 cells transfected with pH19 and T-47D cells transfected with siH19. (B) Measurement of autophagy flux in MDA-231 cells co-transfected with p-mCherry-C1-EGFP-hLC3B and pH19, and T-47D cells co-transfected with p-mCherry-C1-EGFP-hLC3B and siH19. Scale bar, 20 μm. (C) Western blot analysis of autophagy marker expression in MDA-231 cells transfected with Lin28 and T-47D cells transfected with siLin28. (D) RT-qPCR analysis of the RNA expression levels of H19 and Lin28 in T-47D cells transfected with siH19 and let-7 inhibitor. *P<0.05, ***P<0.001 vs. siNC + let-7 inhibitor NC unless otherwise indicated. (E) Western blot analysis of Lin28 expression in T-47D cells transfected with siH19 and let-7 inhibitor. (F) Western blot analysis of autophagy markers expression in T-47D cells transfected with siH19 and let-7 inhibitor. (G) Western blot analysis of autophagy markers expression in T-47D cells transfected with siLin28 and let-7 inhibitor. RT-qPCR analysis of the RNA expression levels of H19, let-7 and Lin28 in MDA-231 cells incubated with (H) 50 μM CQ or (I) 200 nM Rapa. RT-qPCR analysis of the RNA expression levels of H19, let-7 and Lin28 in T-47D cells incubated with (J) 50 μM CQ or (K) 200 nM Rapa. Western blot analysis of Lin28 in T-47D cells incubated with (L) 50 μM CQ or (M) 200 nM Rapa. (N) RT-qPCR analysis of the RNA expression levels of H19 and Lin28 in T-47D cells incubated with 200 nM Rapa and let-7 inhibitor. (O) Western blot analysis of Lin28 in T-47D cells incubated with 200 nM Rapa and let-7 inhibitor. Results represent the mean ± SD of three independent experiments. *P<0.05, **P<0.01. si, small interfering RNA; pH19, pFlag-CMV-H19; RT-qPCR, reverse transcription-quantitative PCR; LC3, light chain 3; CQ, chloroquine; Rapa, rapamycin; NC, negative control; n.s., not significant.

alterations were not associated with changes in the viability of the BC cell lines (Fig. S5).

To further confirm that H19 influenced Lin28 by interacting with let-7 during migration and invasion, pH19mut

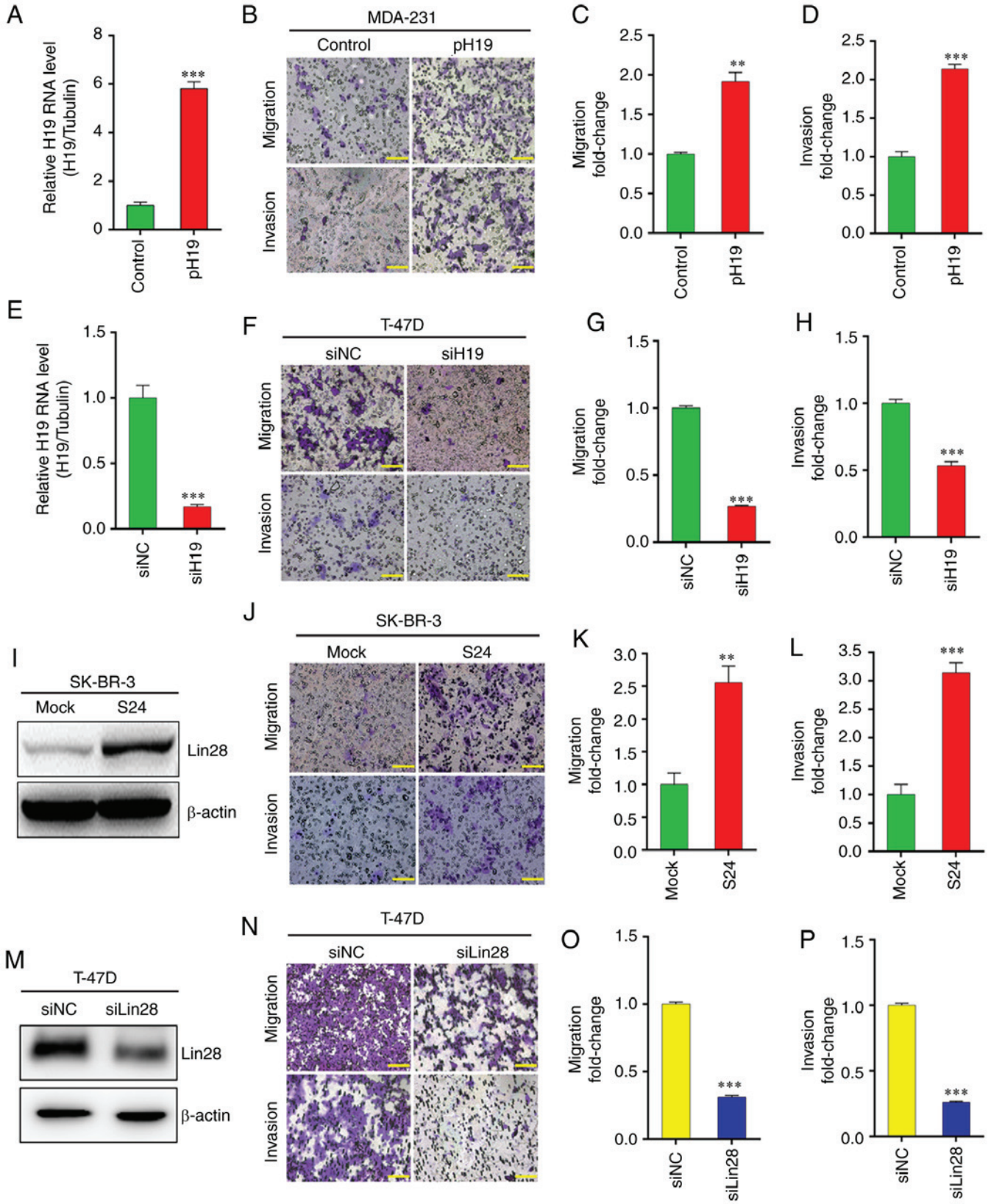

Figure 3. H19 and Lin28 promote migration and invasion of breast cancer cells. (A) H19 overexpression was detected via RT-qPCR. (B) MDA-231 cells were transfected with pH19, and cell migration and invasion were evaluated by Transwell assays. Quantification of (C) migration and (D) invasion rates of the control and pH19 groups. (E) H19 knockdown was detected by RT-qPCR. (F) T-47D cells were transfected with siH19, and cell migration and invasion were evaluated by Transwell assays. Quantification of (G) migration and (H) invasion rates of siNC and siH19 groups. (I) Western blot analysis of Lin28 expression in S24 SK-BR-3 cells. Mock was used as a control. (J) Transwell assays were performed to investigate changes in cell migration and invasion in Mock and S24 cells. Quantification of (K) migration and (L) invasion rates of mock and S24 groups. (M) Lin28 knockdown was detected by western blot analysis. (N) T-47D cells were transfected with siLin28, and cell migration and invasion were evaluated by Transwell assays. Quantification of (O) migration and (P) invasion rates of siCon and siLin28 groups. Scale bar=50 μm. Results represent the mean ± SD of three independent experiments. **P<0.01, ***P<0.001 vs. the corresponding control group. si, small interfering RNA; pH19, pFlag-CMV-H19; RT-qPCR, reverse transcription-quantitative PCR; NC, negative control; S24, SK-BR-3 clone infected with a Lin28 overexpression lentivirus.

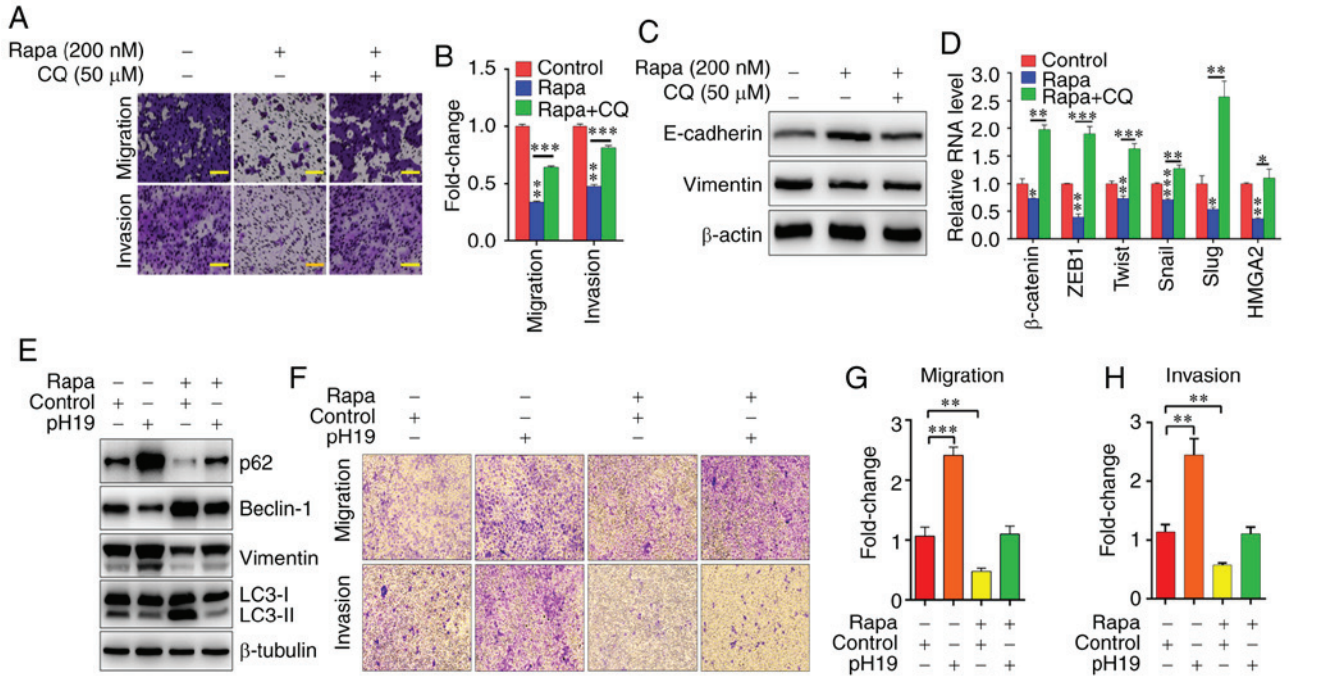

Figure 4. H19/let-7/Lin28 loop regulates the inhibitory effects of autophagy on the EMT of breast cancer cells. (A) T-47D cells were incubated with 200 nM Rapa and 50 μM CQ, and cell migration and invasion were evaluated by Transwell assays. Scale bar=50 μm. (B) Quantification of migration and invasion of T-47D cells incubated with 200 nM Rapa and 50 μM CQ. (C) Western blot analysis of EMT markers. (D) Reverse transcription-quantitative PCR analysis of EMT-inducing transcription factors in T-47D cells incubated with 200 nM Rapa and 50 μM CQ. (E) Western blot analysis of autophagy and EMT markers in T-47D cells treated with 200 nM Rapa and pH19. (F) T-47D cells were treated with 200 nM Rapa and pH19, and cell migration and invasion were evaluated by Transwell assays. Scale bar=50 μm. Quantification of (G) migration and (H) invasion rates of T-47D cells incubated with 200 nM Rapa and pH19. Results represent the mean ± SD of three independent experiments. *P<0.05, **P<0.01, ***P<0.001 vs. Con unless otherwise indicated. pH19, pFlag-CMV-H19; Con, control; CQ, chloroquine; Rapa, rapamycin; EMT, epithelial-mesenchymal transition; ZEB1, zinc finger E-box binding homeobox 1; HMGA2, high-mobility group AT-hook 2; LC3, light chain 3.

was constructed with the let-7 binding site removed (Fig. S6A). Transfection of MDA-231 cells with pH19mut significantly decreased the mRNA expression level of Lin28 (Fig. S6B). Western blot analysis also showed this change in Lin28 expression compared with the control plasmid group (Fig. S6C). Finally, Transwell assays showed that pH19mut suppressed MDA-231 cell migration and invasion (Fig. S6D-F).

Collectively, all above-mentioned results suggested that H19/let-7/Lin28 promotes migration and invasion via EMT in BC cells.

H19/let-7/Lin28 loop regulates EMT-associated genes. EMT is associated with reduced expression of E-cadherin (21); the present study indicated that H19 knockdown led to an increase in the protein expression level of E-cadherin, whereas let-7 inhibitor restored the effect of H19 on its downstream target (Fig. S3C). Several EMT-inducing transcription factors, including β-catenin (22), zinc finger E-box-binding homeobox 1 (23), Twist (24), Snail (25), Slug (26) and high mobility group A2 (27), were reported to act in a gene-specific manner to orchestrate the transcriptional regulation necessary for EMT in various types of tumor, including BC (28); these factors were also found to be associated with H19/let-7/Lin28 in the present study. The results of RT-qPCR verified that H19 knockdown decreased the expression of EMT-inducing transcription factors, and that let-7 inhibitor reversed this effect (Fig. S3D). These observations indicated the involvement of the H19/let-7/Lin28 network in the EMT of BC cells.

H19/let-7/Lin28 loop is involved in the autophagic inhibition of EMT in BC cells. The present study aimed to investigate the role of H19 in the interplay between metastasis and autophagy in BC. First, to determine whether autophagy may inhibit the migration and invasion of BC cells, T-47D cells were treated with Rapa or CQ for 24 h, and the effect on autophagy was evaluated via western blot analysis of p62, beclin-1 and LC3-II (Fig. S7). The results showed that migration and invasion were inhibited by treatment for 24 h with 200 nM Rapa, which was significantly reversed by combined treatment with 50 μM CQ (Fig. 4A and B). EMT-associated proteins and EMT-inducing transcription factors were also investigated; western blotting showed that vimentin was downregulated and E-cadherin was upregulated following incubation with Rapa for 24 h, which was again notably reversed by co-treatment with CQ (Fig. 4C). These results were further verified at the mRNA level by RT-qPCR (Fig. 4D). Finally, a rescue experiment suggested that the overexpression of H19 reversed the reduced migration and invasion that resulted from autophagic inhibition (Fig. 4E-H).

Therefore, the results of the present study suggest that, similar to TGF-β (29), which induces a notable reduction in autophagy via downregulation of beclin-1 and LC3-II and upregulation of p62 (Fig. S8A and B) while enhancing EMT (Fig. S4), H19/let-7/Lin28 may be involved in the interplay between EMT and autophagy.

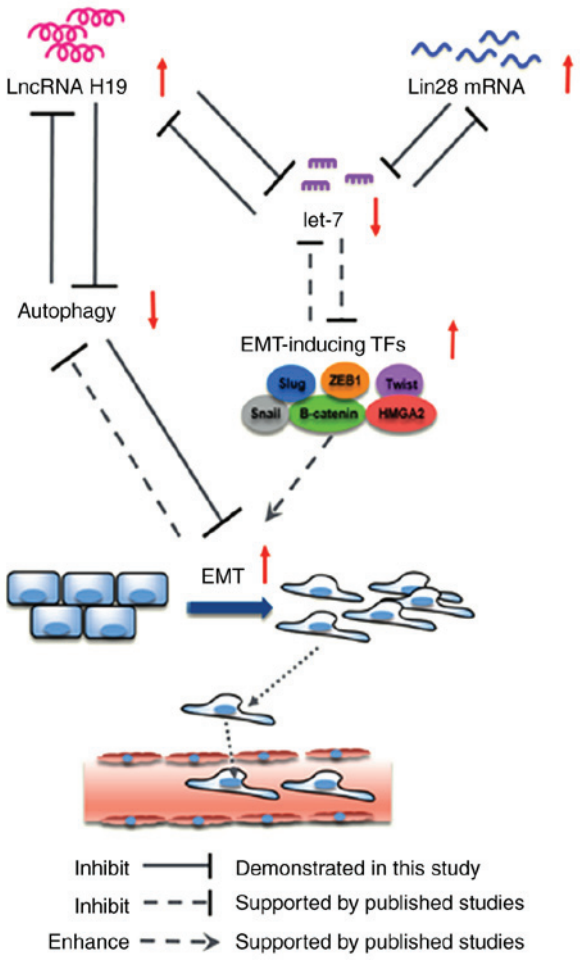

Figure 5. Model of H19/let-7/Lin28 loop inhibiting autophagy and promoting EMT in breast cancer. A proposed regulatory mechanism of the H19/let-7/Lin28 loop inhibiting autophagy and promoting EMT. Black arrows indicate promoting effects; black hammerheads indicate inhibitory effects. Solid lines indicate effects reported in the present study; dotted lines indicate effects reported in previous studies. Red arrows pointing upwards indicate upregulation; red arrows pointing downwards indicate downregulation. LncRNA, long non-coding RNA; EMT, epithelial-mesenchymal transition; TF, transcription factor; ZEB1, zinc finger E-box binding homeobox 1; HMGA2, high-mobility group AT-hook 2.

Discussion

It is well known that lncRNAs are involved in the regulation of complex biological processes via various regulatory mechanisms, which include their interactions with DNA and chromatin, signaling and regulatory proteins, as well as a variety of cellular RNA species. Accumulating evidence has demonstrated the relevance of specific lncRNAs in the initiation and progression of BC (30). A previous study suggested that lncRNAs may act as ceRNAs to communicate with other RNA transcripts via their miRNA response elements (31). For example, lncRNA H19 was found to bind and antagonize the function of miR-17-5p, leading to the expression of tyrosine protein kinase YES1 at both the mRNA and protein level (32).

The lncRNA H19 gene occupies an imprinted region within chromosome 11 (11p15.5), and has been reported to modulate the functions of both miRNAs and proteins (33). Although the mechanism and function of H19 have been studied in various types of cancer, its role in tumor initiation and progression remains the subject of controversy. For example, H19 overexpression increased the metastatic capacity of lung carcinoma (34); however, H19 was also shown to suppress EMT by upregulating the expression of miR-200 family members (35). As an oncogenic regulator in various types of cancer, Lin28 exerts similar biological functions (36,37). In the present study, the overexpression of H19 and Lin28 was shown to promote the migration and invasive ability of BC cells, while H19 and Lin28 knockdown inhibited these functions. Consistent with these findings, the expression of H19 was found to be positively associated with that of Lin28 in BC cell lines. It is therefore proposed that H19 and Lin28 may play oncogenic roles in the progression of BC metastasis.

H19 has been reported to regulate autophagy in numerous types of cancer (38-40). Furthermore, H19 has been revealed to play important roles in promoting tumorigenesis through the stimulation of mTOR signaling (41); this may explain why in the present study, H19 inhibited the Rapa-induced activation of autophagy. This supports previous observations that H19 overexpression promoted mTOR phosphorylation and inhibited autophagic activation in cardiomyocytes (42). As well as mTOR, lncRNAs could also affect the modulation of autophagy-related genes during the autophagic process, in a direct or indirect manner (43). These findings may have importance for the discovery of new mechanisms involved in the interaction of H19 with autophagy.

As for Lin28 and autophagy, as both Lin28 mRNA and protein expression were suppressed by autophagic activation, the same trend was proposed as for H19. There are numerous possible explanations for this. First, the expression of Lin28 was demonstrated to be positively associated with that of H19; thus, it is possible that autophagy could affect the expression of H19 prior to that of Lin28. Additionally, on account of the negative association between let-7 and autophagy, it is speculated that autophagy-related proteins may interact with Lin28 in a direct or indirect manner outside of the H19/let-7/Lin28 ceRNA network. At the same time, in the present study, it was noteworthy that autophagic inhibition or activation could induce significant changes in Lin28 mRNA expression but not protein expression in certain cells; there may be further unknowns to be explored concerning the Lin28 translation process.

There are various possible reasons as to why inducing autophagy could suppress the expression of H19 and Lin28. It has been proposed that tumor-suppressive mechanisms of autophagy contribute to the maintenance of normal bioenergetic functions, oncogene-induced cell death, degradation of oncogenic proteins, immune responses that prevent the establishment and proliferation of malignant cells, anti-inflammatory effects and the maintenance of normal stem cells (44). As, in the present study, autophagic activation or inhibition was revealed to have no significant effect on the expression of let-7, it was proposed that H19 and Lin28 may be involved in other ceRNA networks, or influence other cellular mechanisms.

As the results of the present study suggest that autophagy could inhibit EMT via the H19/let-7/Lin28 network, and as various studies have previously reported other factors associated with both EMT and autophagy (45-47), it is of note that a novel and non-linear relationship links EMT and autophagy in BC. The interplay between these two biological processes can

be influenced by an intricate web of regulatory signaling pathways, which may include the H19/let-7/Lin28 ceRNA network. Other factors may also disrupt the equilibrium between these two processes, such as the overexpression of TGF-β.

EMT is an important cellular mechanism in embryonic development and tissue repair, while also contributing to the progression of various diseases, including cancer (48,49). In addition to genetic alterations, epigenetic regulation also plays a significant role in multiple EMT-related processes, such as the TGF-β, E-cadherin, WNT/β-catenin, Notch, hypoxia and tumor necrosis factor-α pathways (28). With regarding to present research hotspots, studies into EMT tend to focus on lncRNAs and miRNAs. For example, lncRNA metastasis associated lung adenocarcinoma transcript 1, HOX transcript antisense RNA and TRE could represent important examples of lncRNA-mediated regulators of EMT in BC (50). Additionally, let-7 inhibited the Wnt1/Frizzled/β-catenin pathway in hepatocellular carcinoma stem cells (51). Findings such as these and the results of the present study further advance present understanding of the complexity and importance of ceRNA networks during the progression of tumor metastasis.

The complex relationship between autophagy and EMT, and their biological significance in the occurrence and development of cancer, are established. The regulatory crosstalk between autophagy and EMT has been associated with the Ras/Raf1/mitogen-activated protein kinase kinase1/2/ERK (52), JAK/STAT (53), integrin (54) and NF-κB signaling pathways (55).

It is of note that the present study demonstrated interactions among the H19/let-7/Lin28 ceRNA network, EMT and autophagy, and that this feedback loop is critical for BC migration and invasion (Fig. 5). Aberrant molecular events that influence a single element of the loop may trigger a cascade that enhances the metastatic ability of BC cells in the absence of the inducing signal. The precise molecular events involved in the autophagic regulation of H19/let-7/Lin28 require further investigation. However, the present study is an important indicator of the potential interplay of ceRNAs, EMT and autophagy in the diagnosis, prognosis and therapeutic intervention of BC.

Acknowledgements

We thank Professor Xiao-Fang Yu (Cancer Institute, Second Affiliated Hospital, School of Medicine, Zhejiang University) for his critical and informative advice during the revision process.

Funding

The work was supported by the National Natural Science Foundation of China (grant nos. 81972453, 81972597, 81672729 and 81602471) and the Natural Science Foundation of Zhejiang Province (grant nos. LY19H160055, LY19H160059, LY18H160030, LY18H160005 and LY20H160026). It was also sponsored by the Zheng Shu Medical Elite Scholarship Fund.

Availability of data and materials

The datasets used and/or analyzed during the current study are available from the corresponding author on reasonable request.

Authors' contributions

HCX, JGS and ZHC performed all experiments, and were major contributors in writing the manuscript. JJY, BJX and YLJ made contributions to the conception of the study and collected patient samples. UJ, JW, WHZ and SDX analyzed data and revised the manuscript. The study was conceived by LBW and JCZ, who designed and supervised all research and drafted the manuscript. All authors reviewed the final version of the manuscript.

Ethics approval and consent to participate

Informed consent was obtained from all patients. The present study was approved by the Ethics Committee of the Sir Run Run Shaw Hospital affiliated with Zhejiang University, and conducted in full accordance with the ethical principles cited in the World Medical Association Declaration of Helsinki and local legislation.

Patient consent for publication

Not applicable.

Competing interests

The authors declare that they have no competing interests.

References

1. Ganz PA and Goodwin PJ: Breast cancer survivorship: Where are we today? Adv Exp Med Biol 862: 1-8, 2015.
2. Waks AG and Winer EP: Breast cancer treatment: A review. JAMA 321: 288-300, 2019.
3. Zhang X, Li Y, Zhou Y, Mao F, Lin Y, Guan J and Sun Q: Diagnostic performance of indocyanine green-guided sentinel lymph node biopsy in breast cancer: A meta-analysis. PLoS One 11: e0155597, 2016.
4. Rosenberg SM and Partridge AH: Management of breast cancer in very young women. Breast 24 (Suppl 2): S154-S158, 2015.
5. Li CH and Chen Y: Targeting long non-coding RNAs in cancers: Progress and prospects. Int J Biochem Cell Biol 45: 1895-1910, 2013.
6. Bartolomei MS, Zemel S and Tilghman SM: Parental imprinting of the mouse H19 gene. Nature 351: 153-155, 1991.
7. Li X, Lin Y, Yang X, Wu X and He X: Long noncoding RNA H19 regulates EZH2 expression by interacting with miR-630 and promotes cell invasion in nasopharyngeal carcinoma. Biochem Biophys Res Commun 473: 913-919, 2016.
8. Thornton JE and Gregory RI: How does Lin28 let-7 control development and disease? Trends Cell Biol 22: 474-482, 2012.
9. Wang H, Zhao Q, Deng K, Guo X and Xia J: Lin28: An emerging important oncogene connecting several aspects of cancer. Tumour Biol 37: 2841-2848, 2016.
10. Saitoh M: Involvement of partial EMT in cancer progression. J Biochem 164: 257-264, 2018.
11. Guo S, Liang X, Guo M, Zhang X and Li Z: Migration inhibition of water stress proteins from nostoc commune vauch. via activation of autophagy in DLD-1 cells. Int J Biol Macromol 119: 669-676, 2018.
12. Zhou WH, Tang F, Xu J, Wu X, Yang SB, Feng ZY, Ding YG, Wan XB, Guan Z, Li HG, *et al*: Low expression of beclin 1, associated with high Bcl-xL, predicts a malignant phenotype and poor prognosis of gastric cancer. Autophagy 8: 389-400, 2012.
13. Klionsky DJ: Autophagy: From phenomenology to molecular understanding in less than a decade. Nat Rev Mol Cell Biol 8: 931-937, 2007.
14. Liang C, Xu J, Meng Q, Zhang B, Liu J, Hua J, Zhang Y, Shi S and Yu X: TGFB1-induced autophagy affects the pattern of pancreatic cancer progression in distinct ways depending on SMAD4 status. Autophagy 17: 1-15, 2019.

15. Lv Q, Wang W, Xue J, Hua F, Mu R, Lin H, Yan J, Lv X, Chen X and Hu ZW: DEDD interacts with PI3KC3 to activate autophagy and attenuate epithelial-mesenchymal transition in human breast cancer. Cancer Res 72: 3238-3250, 2012.
16. Qin W, Li C, Zheng W, Guo Q, Zhang Y, Kang M, Zhang B, Yang B, Li B, Yang H and Wu Y: Inhibition of autophagy promotes metastasis and glycolysis by inducing ROS in gastric cancer cells. Oncotarget 6: 39839-39854, 2015.
17. Livak KJ and Schmittgen TD: Analysis of relative gene expression data using real-time quantitative PCR and the 2(-Delta Delta C(T)) method. Methods 25: 402-408, 2001.
18. Zhou J, Yang L, Zhong T, Mueller M, Men Y, Zhang N, Xie J, Giang K, Chung H, Sun X, *et al*: H19 lncRNA alters DNA methylation genome wide by regulating S-adenosylhomocysteine hydrolase. Nat Commun 6: 10221, 2015.
19. Wang L, Yuan C, Lv K, Xie S, Fu P, Liu X, Chen Y, Qin C, Deng W and Hu W: Lin28 mediates radiation resistance of breast cancer cells via regulation of caspase, H2A.X and Let-7 signaling. PLoS One 8: e67373, 2013.
20. Kallen AN, Zhou XB, Xu J, Qiao C, Ma J, Yan L, Lu L, Liu C, Yi JS, Zhang H, *et al*: The imprinted H19 lncRNA antagonizes let-7 microRNAs. Mol Cell 52: 101-112, 2013.
21. Gonzalez DM and Medici D: Signaling mechanisms of the epithelial-mesenchymal transition. Sci Signal 7: re8, 2014.
22. Wu ZQ, Li XY, Hu CY, Ford M, Kleer CG and Weiss SJ: Canonical Wnt signaling regulates Slug activity and links epithelial-mesenchymal transition with epigenetic breast cancer 1, early onset (BRCA1) repression. Proc Natl Acad Sci USA 109: 16654-16659, 2012.
23. Rhodes LV, Tate CR, Segar HC, Burks HE, Phamduy TB, Hoang V, Elliott S, Gilliam D, Pounder FN, Anbalagan M, *et al*: Suppression of triple-negative breast cancer metastasis by pan-DAC inhibitor panobinostat via inhibition of ZEB family of EMT master regulators. Breast Cancer Res Treat 145: 593-604, 2014.
24. Yang J, Hou Y, Zhou M, Wen S, Zhou J, Xu L, Tang X, Du YE, Hu P and Liu M: Twist induces epithelial-mesenchymal transition and cell motility in breast cancer via ITGB1-FAK/ILK signaling axis and its associated downstream network. Int J Biochem Cell Biol 71: 62-71, 2016.
25. Yook JI, Li XY, Ota I, Hu C, Kim HS, Kim NH, Cha SY, Ryu JK, Choi YJ, Kim J, *et al*: A Wnt-Axin2-GSK3beta cascade regulates snail1 activity in breast cancer cells. Nat Cell Biol 8: 1398-1406, 2006.
26. Weyemi U, Redon CE, Sethi TK, Burrell AS, Jailwala P, Kasoji M, Abrams N, Merchant A and Bonner WM: Twist1 and Slug mediate H2AX-regulated epithelial-mesenchymal transition in breast cells. Cell Cycle 15: 2398-2404, 2016.
27. Zou Q, Wu H, Fu F, Yi W, Pei L and Zhou M: RKIP suppresses the proliferation and metastasis of breast cancer cell lines through up-regulation of miR-185 targeting HMGA2. Arch Biochem Biophys 610: 25-32, 2016.
28. Felipe Lima J, Nofech-Mozes S, Bayani J and Bartlett JM: EMT in breast carcinoma-a review. J Clin Med 5: E65, 2016.
29. Lamouille S, Connolly E, Smyth JW, Akhurst RJ and Derynck R: TGF-β-induced activation of mTOR complex 2 drives epithelial-mesenchymal transition and cell invasion. J Cell Sci 125: 1259-1273, 2012.
30. Wang J, Ye C, Xiong H, Shen Y, Lu Y, Zhou J and Wang L: Dysregulation of long non-coding RNA in breast cancer: An overview of mechanism and clinical implication. Oncotarget 8: 5508-5522, 2017.
31. Salmena L, Poliseno L, Tay Y, Kats L and Pandolfi PP: A ceRNA hypothesis: The Rosetta Stone of a hidden RNA language? Cell 146: 353-358, 2011.
32. Liu L, Yang J, Zhu X, Li D, Lv Z and Zhang X: Long noncoding RNA H19 competitively binds miR-17-5p to regulate YES1 expression in thyroid cancer. FEBS J 283: 2326-2339, 2016.
33. Imig J, Brunschweiger A, Brümmer A, Guennewig B, Mittal N, Kishore S, Tsikrika P, Gerber AP, Zavolan M and Hall J: miR-CLIP capture of a miRNA targetome uncovers a lincRNA H19-miR-106a interaction. Nat Chem Biol 11: 107-114, 2015.
34. Matouk IJ, Raveh E, Abu-lail R, Mezan S, Gilon M, Gershtain E, Birman T, Gallula J, Schneider T, Barkali M, *et al*: Oncofetal H19 RNA promotes tumor metastasis. Biochim Biophys Acta 1843: 1414-1426, 2014.
35. Zhang L, Yang F, Yuan JH, Yuan SX, Zhou WP, Huo XS, Xu D, Bi HS, Wang F and Sun SH: Epigenetic activation of the MiR-200 family contributes to H19-mediated metastasis suppression in hepatocellular carcinoma. Carcinogenesis 34: 577-586, 2013.
36. Balzeau J, Menezes MR, Cao S and Hagan JP: The LIN28/let-7 pathway in cancer. Front Genet 8: 31, 2017.
37. Jiang S and Baltimore D: RNA-binding protein Lin28 in cancer and immunity. Cancer Lett 375: 108-113, 2016.
38. Cui C, Li Z and Wu D: The long non-coding RNA H19 induces hypoxia/reoxygenation injury by up-regulating autophagy in the hepatoma carcinoma cells. Biol Res 52: 32, 2019.
39. Wang M, Han D, Yuan Z, Hu H, Zhao Z, Yang R, Jin Y, Zou C, Chen Y, Wang G, *et al*: Long non-coding RNA H19 confers 5-Fu resistance in colorectal cancer by promoting SIRT1-mediated autophagy. Cell Death Dis 9: 1149, 2018.
40. Wang J, Xie S, Yang J, Xiong H, Jia Y, Zhou Y, Chen Y, Ying X, Chen C, Ye C, *et al*: The long noncoding RNA H19 promotes tamoxifen resistance in breast cancer via autophagy. J Hematol Oncol 12: 81, 2019.
41. Zhang J, Liu CY, Wan Y, Peng L, Li WF and Qiu JX: Long non-coding RNA H19 promotes the proliferation of fibroblasts in keloid scarring. Oncol Lett 12: 2835-2839, 2016.
42. Zhuo C, Jiang R, Lin X and Shao M: LncRNA H19 inhibits autophagy by epigenetically silencing of DIRAS3 in diabetic cardiomyopathy. Oncotarget 8: 1429-1437, 2017.
43. Xu Z, Yan Y, Qian L and Gong Z: Long non-coding RNAs act as regulators of cell autophagy in diseases (review). Oncol Rep 37: 1359-1366, 2017.
44. Galluzzi L, Pietrocola F, Bravo-San Pedro JM, Amaravadi RK, Baehrecke EH, Cecconi F, Codogno P, Debnath J, Gewirtz DA, Karantza V, *et al*: Autophagy in malignant transformation and cancer progression. EMBO J 34: 856-880, 2015.
45. Guo Q, Jing FJ, Xu W, Li X, Li X, Sun JL, Xing XM, Zhou CK and Jing FB: Ubenimex induces autophagy inhibition and EMT suppression to overcome cisplatin resistance in GC cells by perturbing the CD13/EMP3/PI3K/AKT/NF-κB axis. Aging 11: 2019.
46. Liang F, Ren C, Wang J, Wang S, Yang L, Han X, Chen Y, Tong G and Yang G: The crosstalk between STAT3 and p53/RAS signaling controls cancer cell metastasis and cisplatin resistance via the Slug/MAPK/PI3K/AKT-mediated regulation of EMT and autophagy. Oncogenesis 8: 59, 2019.
47. Han LL, Jia L, Wu F and Huang C: Sirtuin6 (SIRT6) promotes the EMT of hepatocellular carcinoma by stimulating autophagic degradation of E-cadherin. molecular cancer research: Mol Cancer Res 17: 2267-2280, 2019.
48. Takahashi K, Tanabe K, Ohnuki M, Narita M, Ichisaka T, Tomoda K and Yamanaka S: Induction of pluripotent stem cells from adult human fibroblasts by defined factors. Cell 131: 861-872, 2007.
49. Jiang Z, Jones R, Liu JC, Deng T, Robinson T, Chung PE, Wang S, Herschkowitz JI, Egan SE, Perou CM and Zacksenhaus E: RB1 and p53 at the crossroad of EMT and triple-negative breast cancer. Cell Cycle 10: 1563-1570, 2011.
50. Dhamija S and Diederichs S: From junk to master regulators of invasion: lncRNA functions in migration, EMT and metastasis. Int J Cancer 139: 269-280, 2016.
51. Jin B, Wang W, Meng XX, Du G, Li J, Zhang SZ, Zhou BH and Fu ZH: Let-7 inhibits self-renewal of hepatocellular cancer stem-like cells through regulating the epithelial-mesenchymal transition and the Wnt signaling pathway. BMC Cancer 16: 863, 2016.
52. Qiu XY, Hu DX, Chen WQ, Chen RQ, Qian SR, Li CY, Li YJ, Xiong XX, Liu D, Pan F, *et al*: PD-L1 confers glioblastoma multiforme malignancy via Ras binding and Ras/Erk/EMT activation. Biochim Biophys Acta Mol Basis Dis 1864: 1754-1769, 2018.
53. Hu F, Zhao Y, Yu Y, Fang JM, Cui R, Liu ZQ, Guo XL and Xu Q: Docetaxel-mediated autophagy promotes chemoresistance in castration-resistant prostate cancer cells by inhibiting STAT3. Cancer Lett 416: 24-30, 2018.
54. Sosa P, Alcalde-Estevez E, Plaza P, Troyano N, Alonso C, Martínez-Arias L, Evelem de Melo Aroeira A, Rodriguez-Puyol D, Olmos G, López-Ongil S and Ruíz-Torres MP: Hyperphosphatemia promotes senescence of myoblasts by impairing autophagy through Ilk overexpression, a possible mechanism involved in sarcopenia. Aging Dis 9: 769-784, 2018.
55. Huang M and Xin W: Matrine inhibiting pancreatic cells epithelial-mesenchymal transition and invasion through ROS/NF-κB/MMPs pathway. Life Sci 192: 55-61, 2018.